



Performance of low-salinity water flooding for enhanced oil recovery improved by SiO₂ nanoparticles

Tangestani Ebrahim¹ · Vafaie Sefti Mohsen¹ · Shadman Mohammad Mahdi¹ · Kazemi Tooseh Esmaeel¹ · Ahmadi Saeb¹

Received: 18 November 2017 / Published online: 10 January 2019
© The Author(s) 2019

Abstract

Low-salinity water injection has been utilized as a promising method for oil recovery in recent years. Low-salinity water flooding changes the ion composition or brine salinity for improving oil recovery. Recently, the application of nanoparticles with low-salinity water flooding has shown remarkable results in enhanced oil recovery (EOR). Many studies have been performed on the effect of nanofluids on EOR mechanisms. Their results showed that nanofluids can improve oil recovery when used in low-salinity water flooding. In this work, the effects of injection of low-salinity water and low-salinity nanofluid (prepared by adding SiO₂ nanoparticles to low-salinity water) on oil recovery were investigated. At first, the effects of ions were investigated with equal concentrations in low-salinity water flooding. The experimental results showed that the monovalent ions had better performance than the divalent ions because of them having more negative zeta potential and less ionic strength. Also, low-salinity water flooding recovered 6.1% original oil in place (OOIP) more than the high-salinity flooding. Contact angle measurements demonstrated that low-salinity water could reduce the contact angle between oil and water. Then in the second stage, experiments were continued by adding SiO₂ nanoparticles to the K⁺ solution which had the highest oil recovery at the first stage. The experimental results illustrated that the addition of SiO₂ nanoparticles up to 0.05 wt% increased oil recovery by about 4% OOIP more than the low-salinity water flooding.

Keywords Enhanced oil recovery · Low-salinity water · Low-salinity nanofluid · Zeta potential

1 Introduction

Low-salinity water (LSW) flooding has been suggested as an effective method for enhancing oil recovery (EOR) in sandstone reservoirs when the salinity of the injection fluids is between 1400 and 5000 ppm (Alotaibi et al. 2010; Austad et al. 2010; Buikema et al. 2011; Hilner et al. 2015; Lager et al. 2008b; Morrow and Buckley 2011; Piñerez Torrijos et al. 2016; Qiao et al. 2016; Vledder et al. 2010) and although most of the experiments were done below 100 °C, there appeared to be no limitation on temperature (Lager et al. 2008a). Low-salinity water flooding may be considerably effective in special conditions and is recommended for

increasing oil recovery when the following are encountered: clay must be present in the sandstones, polar components (acidic and/or basic material) present in crude oil, and formation water must contain divalent ions like Ca²⁺ (Lager et al. 2007; Tang and Morrow 1999).

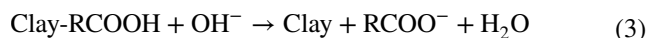
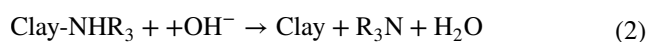
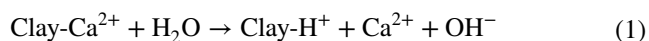
The mechanisms suggested in low-salinity water flooding include: double-layer expansion between fine particles and limited fines release (LFR) with a change in wettability toward water wetness resulting from the removal of the mixed wet fines (Tang and Morrow 1999), double-layer expansion between oil/rock contact areas (Ligthelm et al. 2009; Matthiesen et al. 2014; Nasralla and Nasr-El-Din, 2014; Xie et al. 2014), and multi-component ion exchange (MIE) (Lager et al. 2007).

Austad et al. proposed that organic materials desorbing from the clay surface occurred because of an increase in pH at the clay-water interface. The increase in pH is due to desorption of cations from the surface during low-salinity water flooding. The proposed mechanism is schematically illustrated by Austad et al. (2010).

Edited by Yan-Hua Sun

✉ Tangestani Ebrahim
ebrahim_tangestani@yahoo.com

¹ Chemical Engineering Department, Tarbiat Modares University, 116-14115, Tehran, Iran



Nowadays, nanoparticles are widely used to improve the performance of chemical and physical processes in many fields, including petroleum engineering. Nanoparticle-assisted low-salinity water flooding embraces both nanoparticles and ions as EOR agents in the injection water. Materials having a dimension of 100 nm or less are called ‘nanoparticles’ (Das et al. 2008). They are composed of two parts: a core and a thin shell (Das et al. 2008). Previous studies suggested enhanced characteristics of nanoparticles including very high specific surface area, remarkable thermal features, and chemical capability to modify the wetting characteristics of reservoir rocks and the rheological properties of drilling fluids (Arab et al. 2014; Ayatollahi and Zerafat 2012; Baird and Walz 2007; Hendraningrat and Torsæter 2014; Huang et al. 2008; Li et al. 2016; Pourafshary et al. 2009; Rahbar et al. 2010; Timofeeva et al. 2011; Zamani et al. 2010; Zhang et al. 2010). Moreover, nanoparticles are used as an EOR agent to alter water properties such as viscosity; this allows for higher mobility of the injected fluids in order to release the trapped oil (Ayatollahi and Zerafat 2012).

One of the main mechanisms in nanofluid-assisted flooding is called the structural disjoining pressure (Chengara et al. 2004; Wasan et al. 2011; Wasan and Nikolov 2003). This mechanism deals with the energy existing between nanoparticles that leads to Brownian motion and electrostatic repulsion between them. As the nanoparticle size becomes smaller, the electrostatic repulsion force between nanoparticles will be larger. The larger the number of the nanoparticles, the bigger the force will be (Mcelfresh et al. 2012).

The presence of these nanoparticles in the three-phase contact region causes a creation of a wedge-film structure. Structural disjoining pressure is correlated to the fluid’s ability to spread along the surface of a substrate because of an imbalance of the interfacial forces among the solid, oil, and aqueous phases (Chengara et al. 2004). The wedge film can separate the formation fluids (oil, water, and gas) from the formation’s surface, thereby recovering more fluids (Mcelfresh et al. 2012).

Beside this mechanism, the surface modification of porous media in contact with nanoparticles should be considered. Nanoparticles would increase the attractive force in the surface of porous media, so clay minerals cannot detach from the surface (Arab and Pourafshary 2013).

In this work, the effects of low-salinity water and a combination of nanoparticles with low-salinity water injection on oil recovery were studied. Finally, the recovery mechanism was discussed using multiple analyses such as IFT, contact angle, zeta potential, and viscosity.

2 Experimental

2.1 Material

The brines used were artificially prepared by dissolving desired amounts of salts in distilled water. NaCl, KCl, MgCl₂, and CaCl₂ used here were obtained from Merck. As Table 1 shows, the concentrations of all ions in low-salinity brines were the same at 0.03422 mol/L.

The crude oil used in this study had an API gravity of 24° and a specific gravity of 0.89. The viscosity of the crude oil was 29 cP at ambient temperature.

Silicon dioxide (SiO₂) nanoparticles with 99.99% purity were purchased from the TECNAN Company, and their physical properties are reported in Table 2.

Table 1 Concentration of ions in brines

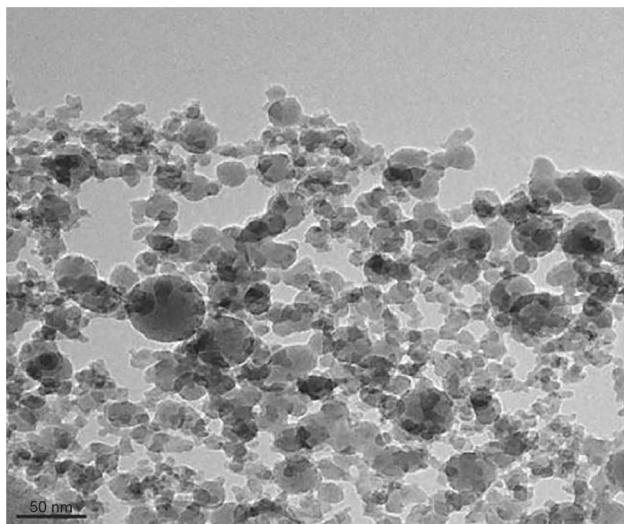
Brines	Ion concentration, mol/L				Total dissolved solids (TDS), ppm	Water type
	Na ⁺	K ⁺	Ca ²⁺	Mg ²⁺		
Brine 1	0.18021	0	0.5133	0	50,000	High salinity
Brine 2	0.03422	0	0	0	2000	Low salinity
Brine 3	0	0.03422	0	0	2585	Low salinity
Brine 4	0	0	0	0.03422	3258	Low salinity
Brine 5	0	0	0.03422	0	3795	Low salinity

Table 2 Properties of SiO₂ nanoparticles

Average particle size, nm	Specific surface area (SSA), m ² /g	True density, cm ³ /g	Pore volume, cm ³ /g	Average pore size, Å	Morphology	Color
10–15	180–270	2.22	0.549	110.13	Spherical	White

Table 3 Concentration of SiO₂ nanoparticles in low-salinity nanofluids

Nanofluids	SiO ₂ concentration, wt%	K ⁺ concentration, mol/L	TDS, ppm
6	0.02	0.03422	2585
7	0.05	0.03422	2585
8	0.08	0.03422	2585
9	0.10	0.03422	2585

**Fig. 1** TEM image of SiO₂ nanoparticles (with a diameter of 10–15 nm)

Low-salinity SiO₂ nanofluids were formulated by sonicating SiO₂ nanoparticles in Brine 3 using a 400-watt ultrasonic homogenizer; the concentrations of SiO₂ nanoparticles and ion compositions are listed in Table 3.

The microscopic structure of dry SiO₂ nanoparticles was observed with a transmission electron microscope (TEM), as shown in Fig. 1.

In experiments, the sand packs used were 7.62 cm long, by 3.81 cm in diameter, filled with 90% glass beads with a diameter of 210–600 μm and 10% kaolinite clay. The porosity and permeability values of each sand pack used are given in the following section.

2.2 Zeta potential

Zeta potential (ζ) values of SiO₂ nanofluids were measured with a Malvern Zen 3600 (Malvern Instruments, UK) using the electrophoresis method. In this method, a fluid sample containing suspended particles is influenced by the electric field. As a result, the charged particles in the zeta potential and intensity of the applied electric field with different speeds are attracted toward the oppositely charged

electrodes. By measuring the speed of the particles moving in the porous media, the zeta potential of the particles is measured. At first, two sets of samples were prepared for brines 2, 3, 4, and 5; then, glass beads were equally added to the first set of samples and clay was added to the next set. After standing for 24 h, the zeta potentials of the solutions were measured.

2.3 Contact angle

The effects of low-salinity water and low-salinity nanofluids (adding SiO₂ nanoparticles to low-salinity water) on wettability alteration were investigated by measuring the contact angle between crude oil and brines or nanofluids on glass plates. Contact angle measurements were performed at room temperature and atmospheric pressure with a Kruss DSA-100 contact angle analyzer with an accuracy of $\pm 0.1^\circ$. Measurements were conducted on glass plates because glass is of the same material as glass beads filled in sand packs. After being cleaned with acetone, 18 pieces of glass plate were immersed in brines at 333 K for 1 h to form a film of brine on the glass plates. The glass plates were then aged in crude oil at 333 K for 4 weeks. In order to measure the contact angle, the oil-wetted glass plate was immersed in the low-salinity water or the low-salinity nanofluid. Then, a crude oil drop was placed on the plate surface.

The measurements were performed for two sets of the plates, each containing 9 plates. The contact angles of the first 9 plates were measured at the initial stage of putting the oil-wetted plates in brines, and the contact angles of the second set were measured after remaining in contact with the brines for 24 h. In order to better clarify the results, the contact angles were measured in three different spots on the surface of each glass plate, and the average value was reported as the contact angle of that sample.

2.4 Interfacial tension

The IFT between crude oil and aqueous solutions was measured using the ring method with a Sigma 700 force tensiometer. All measurements were performed in ambient conditions. Brine and crude oil were added to the device, and the IFT was measured. In this method, a platinum ring is held at the interface of water and oil. The force required to pull the ring out of the interface is related to the IFT.

2.5 Fluid viscosity

Viscosity was measured with a Brookfield rotational viscometer (model NDJ-4) in ambient conditions. This instrument

can be used to determine viscosity resistance and dynamic viscosity of liquids in a wide range.

2.6 Core flooding procedure

The core flood setup consisted of a high-pressure positive displacement pump, two transfer vessels, a hydraulic pump, a core holder, and a heater, as illustrated in Fig. 2. Flooding procedures are as follows:

(1) Five pore volume (PV) of synthetic brine was injected at a rate of $0.1 \text{ cm}^3/\text{min}$ to ensure that the sand pack was fully saturated with water. Then, the core permeability was measured at several injection rates. (2) Crude oil was injected into the sand pack until no water was produced from the sand pack. (3) The sand pack was kept at this situation and aged at 333 K for 4 weeks. (4) Brine was injected into the sand pack at a flow rate of $0.1 \text{ cm}^3/\text{min}$ until no oil was produced, and the oil recovery was calculated.

3 Results and discussion

The experiments include two parts: first, low-salinity water flooding was performed in order to choose the best ion and to optimize its concentration. In the second part, SiO_2 nanoparticles were added to the selected low-salinity water to study its effect on oil recovery.

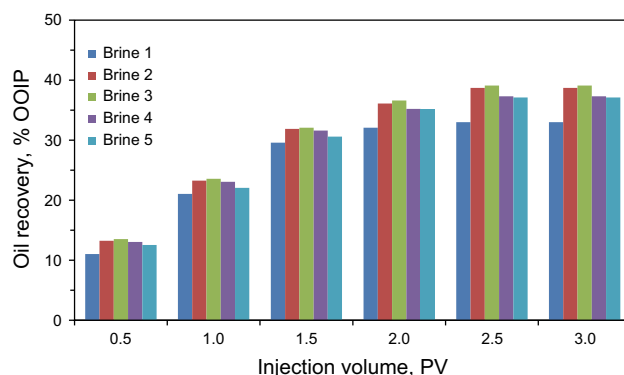


Fig. 3 Oil recovery versus cumulative volume of brine injected into the sand pack, brines 2–5 were low-salinity water of an ion concentration of 0.03422 mol/L

3.1 Effect of low-salinity water flooding on oil recovery

Mg^{2+} , Ca^{2+} , K^+ , and Na^+ ions were tested to determine the best ion for increasing oil recovery. As a result, the maximum oil recovery of low-salinity water injection was about 39% which is 6.1% more than high-salinity brine injection. It can be seen from Fig. 3 that K^+ and Na^+ had better effects on oil recovery than did Mg^{2+} and Ca^{2+} . The kaolinite clay used here did not swell significantly in contact with brine, but there was some unusual pressure drop at core ends. This is due to clay migration during brine injection. Monovalent ions tended to detach the charged clay particles from rock surfaces and higher pressure drop occurred in monovalent-ion brine injection. The detached clay particles entered bulk of the fluid and flowed inside

Fig. 2 Schematic of the setup used for core displacement

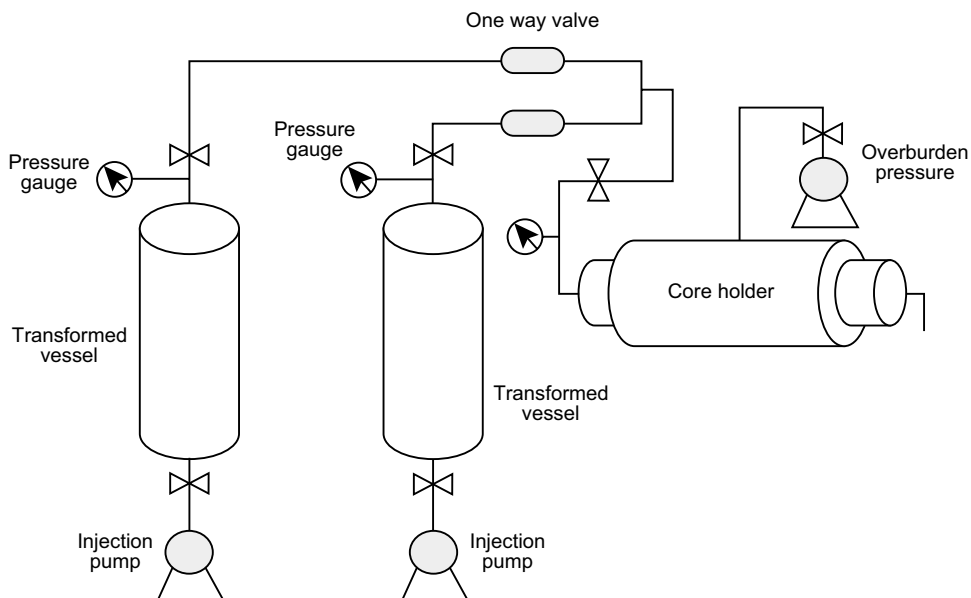


Table 4 Pressure drop across the sand pack and oil recovery in brine displacement tests

Displacement fluid	Sand pack porosity, %	Sand pack permeability, mD	Pressure drop, psi	Final oil recovery by water flooding, % OOIP	Incremental oil recovery compared to high-salinity water flooding (Brine 1), % OOIP
Brine 1	29	–	–	32.9	–
Brine 2	30	51.3	0.32	38.6	5.7
Brine 3	30	46.8	0.35	39.0	6.1
Brine 4	31	56.6	0.29	37.2	4.3
Brine 5	31	60.8	0.27	37.0	4.1

Table 5 Values of zeta potential for low-salinity water

Water	Ion in brine	Zeta potential of clay, mV	Zeta potential of glass bead, mV	Ionic strength, mol/L
Brine 2	Na ⁺	–26.5	–27.4	0.03422
Brine 3	K ⁺	–28.4	–29.8	0.03422
Brine 4	Ca ²⁺	–8.6	–11.0	0.10266
Brine 5	Mg ²⁺	–8.0	–10.0	0.10266

Table 6 IFT values between low-salinity water and crude oil

Water	Measured IFT, mN/m
Distilled water	21.0
Brine 1	28.2
Brine 2	21.2
Brine 3	21.1
Brine 4	21.1
Brine 5	21.2

porous media until reaching pore throats. These particles would plug the throats, and as a result a higher pressure drop was recorded at the core ends. This is one of the assisting EOR mechanisms in low-salinity water flooding. The pressure drop data and the ultimate oil recovery are shown in Table 4.

3.1.1 Effect of low-salinity water on zeta potential

As mentioned above, one of the mechanisms of low-salinity water flooding is double-layer expansion. Ligthelm et al. (2009) introduced double-layer expansion between clay surface and oil particles as one of the governing mechanisms in low-salinity water flooding that leads to lowering the zeta potential toward more negative values. Also by lowering the salinity in the brine, the ionic strength decreases and the electrostatic repulsion between clay particles and oil increases (Ligthelm et al. 2009).

The ionic strength is defined as:

$$I = \frac{1}{2} \sum_{i=1}^n C_i Z_i^2$$

where *C* is molality, mol/kg; *Z* is ion capacity.

The obtained results showed that the glass bead or the clay sample which was exposed to K⁺ and Na⁺ had more negative zeta potential values than the sample exposed to Mg²⁺ and Ca²⁺ (Table 5). So, K⁺ and Na⁺ are more effective on oil recovery than Mg²⁺ and Ca²⁺ because of lower ionic

strength and more negative zeta potential. Table 5 shows the zeta potential values of four types of low-salinity water.

3.1.2 Effect of low-salinity water on IFT

The IFTs between low-salinity water and crude oil are listed in Table 6, and the IFT value between distilled water and crude oil is also listed to compare the effect of ions. The experimental results showed that the ion in the low-salinity water reduced the IFT between water and crude oil from 28.2 to approximately 21.1 mN/m². Also, the IFT reduced in low-salinity cases compared to the high-salinity brine (Brine 1). The value of IFT was nearly the same for both monovalent and divalent ions. This leads to more oil recovery, as the IFT between oil and brine decreases, more oil will be produced from the sand pack.

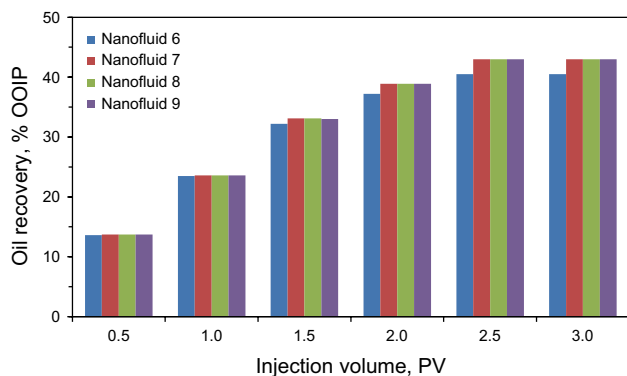
3.1.3 Effect of low-salinity water on contact angle

Contact angle measurements were performed to determine the mechanism of low-salinity water flooding, and the contact angle values are listed in Table 7.

As can be seen from Table 7, the low-salinity water could reduce the contact angle more than the high-salinity water. It can be concluded that the low-salinity water may alter wettability toward more water wetness and as a result the oil recovery increases. According to the results of zeta potential, oil recovery, IFT, and contact angle measurements, K⁺ brine was selected as the best cation for enhanced oil recovery and

Table 7 Contact angle values for brines 1–5

Brine	Ion in brine	Contact angle at the initial state, degree	Contact angle after in contact with brine for 24 h, degree	Percentage changes after in contact with brine for 24 h
Brine 1	Na ⁺ , Ca ²⁺ (high-salinity water)	51.0	47.3	−7.3
Brine 2	Na ⁺	44.3	38.3	−13.5
Brine 3	K ⁺	44.0	38.3	−12.8
Brine 4	Mg ²⁺	44.2	39.3	−11.1
Brine 5	Ca ²⁺	44.7	39.6	−11.3

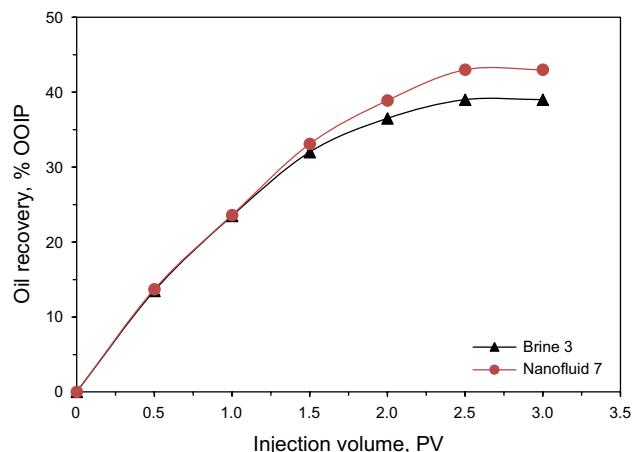
**Fig. 4** Oil recovery enhanced by nanofluids (nanofluids 6–9)

the rest of the experiments were performed in the presence of this ion and SiO₂ nanoparticles.

3.2 Effect of nanoparticles in low-salinity water on enhanced oil recovery

SiO₂ nanoparticles were added to Brine 3 to prepare nanofluids of different nanoparticle concentrations (0.02 wt%, 0.05 wt%, 0.08 wt%, and 0.1 wt%, respectively). The oil recovery increased as the SiO₂ nanoparticle concentration increased up to 0.05 wt%, and there was no further increase above this concentration. The ultimate oil recovery was about 43% at 2.5 PV nanofluid injection; above this volume there was no further increase in oil recovery. Figure 4 shows the SiO₂ nanofluid flooding results. The following mechanisms may be the reason for oil recovery enhanced by increasing the nanoparticle concentration up to 0.05 wt%. Four different physical mechanisms commonly cause the particles to be retained in the pores: (1) log-jamming, (2) mechanical entrapment, (3) gravity settling, and (4) adsorption.

It should be considered that nanofluid flooding would not always increase oil recovery because various physical mechanisms commonly cause the particles to be retained in the pores (Engeset 2012):

**Fig. 5** Comparison of oil recovery enhanced by low-salinity water (Brine 3 containing K⁺) and low-salinity nanofluid (containing K⁺ + SiO₂ nanoparticles)

1. Adsorption of nanoparticles on the surface of the porous rock due to Brownian motion of nanoparticles and their electrostatic interactions.
2. Mechanical entrapment of nanoparticles when the particle sizes are larger than pore throats.
3. Sedimentation or gravity settling when the densities of the moving particles and the carrying fluid are very different.
4. Log-jamming when the nanoparticles move at lower velocities compared to the carrying fluid and accumulate in the pore throats, which eventually leads to blockage.

As illustrated in Fig. 5 and Table 8, the addition of SiO₂ nanoparticles to the low-salinity water would increase the oil recovery. This proves the effectiveness of SiO₂ nanoparticles as an EOR agent. The pressure drop data are shown in Table 8.

3.2.1 Effect of nanoparticles in low-salinity water on brine viscosity

As shown in Fig. 6, the addition of SiO₂ nanoparticles to low-salinity water would increase the viscosity of brine;

Table 8 Pressure drop across the sand pack in nanofluid displacement tests

Displacement fluid	K ⁺ concentration, mol/L	SiO ₂ nanoparticle concentration, wt%	Sand pack porosity, %	Sand pack permeability, mD	Pressure drop, psi	Final oil recovery by water flooding, % OOIP	Incremental oil recovery compared to high-salinity water flooding, % OOIP
Nanofluid 6	0.03422	0.02	32	44.5	0.36	40.5	7.6
Nanofluid 7	0.03422	0.04	29	42.0	0.39	43.0	10.1
Nanofluid 8	0.03422	0.08	30	41.4	0.39	43.0	10.1
Nanofluid 9	0.03422	0.10	31	40.0	0.41	43.0	10.1
Brine 3	0.03422	0	30	46.8	0.35	39.0	6.1

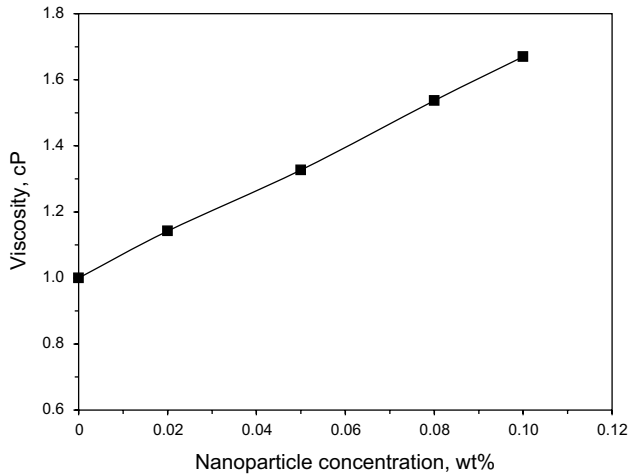


Fig. 6 Brine viscosity after the addition of SiO₂ nanoparticles

however, the viscosity increase was not significant, and the mobility of the nanofluid decreased more than the low-salinity water. It can be concluded that increasing viscosity of the displacing fluid (nanofluid) would drive more oil toward production, and finally, the oil recovery is higher than low-salinity water flooding.

3.2.2 Effect of SiO₂ nanoparticles in low-salinity water on IFT

In order to study the effect of SiO₂ nanoparticles in the low-salinity water on IFT, four tests were conducted and the experimental results are listed in Table 9. The results showed that the addition of SiO₂ nanoparticles to the low-salinity water could not alter the IFT between brine and crude oil, and the IFT value was approximately 21.1 mN/m² for any concentration of SiO₂ nanoparticles.

Table 9 IFT values between nanofluids and crude oil

Fluid	Measured IFT, mN/m
Distilled water	21.0
Brine 3	21.1
Nanofluid 6	20.3
Nanofluid 7	21.2
Nanofluid 8	21.2
Nanofluid 9	21.2

3.2.3 Effect of SiO₂ nanoparticles in low-salinity water on contact angle

Contact angle measurements were performed to determine the mechanism of EOR after adding SiO₂ nanoparticles to the low-salinity water. The obtained contact angle values are listed in Table 10.

Measurements show that increasing the concentration of SiO₂ nanoparticles increased the water wetness of the glass surface. This is because, when the number of SiO₂

Table 10 Contact angle values for the nanofluids

Nanofluid	SiO ₂ nanoparticle concentration, wt%	Contact angle at the initial stage, degree	Contact angle after in contact with nanofluid for 24 h, degree	Percentage changes after in contact with brine 24 h
Nanofluid 6	0.02	39.4	36.2	−8.26
Nanofluid 7	0.05	38.5	35.3	−8.4
Nanofluid 8	0.08	36.4	32.4	−11.1
Nanofluid 9	0.10	34.6	30.5	−11.7

nanoparticles increases, the electrostatic repulsive force between nanoparticles becomes larger. As a result, driven by the aqueous pressure of the bulk liquid, the nanofluid will spread along the solid surface thus decreasing the contact angle which enhances the water wetness of the surface.

As shown in Table 10, adding SiO₂ nanoparticles to the low-salinity water could reduce the contact angle more than that of the low-salinity water itself. It can be concluded that the addition of SiO₂ nanoparticles to the low-salinity water can alter contact angle.

4 Conclusions

Previous studies have reported the effectiveness of low-salinity water flooding on enhanced oil recovery. The experimental results of this study showed that the low-salinity water flooding would increase the oil recovery and the addition of SiO₂ nanoparticles to the low-salinity water improved the oil recovery even more than low-salinity water alone. At the first set of experiments, the low-salinity water flooding was performed by using brines containing Na⁺, K⁺, Ca²⁺, and Mg²⁺, respectively, and the recovery was recorded between 33% and 39%. On the basis of oil recovery and zeta potential values, brine containing K⁺ was chosen as the most effective ion for EOR. Zeta potential analysis showed that the monovalent ions had better performance than the divalent ions because of having a more negative zeta potential and lower ionic strength. Also, the low-salinity water reduced the IFT between the solution and oil. The second set of experiments were performed by combining SiO₂ nanoparticles and K⁺ brine. SiO₂ nanoparticles were added to the K⁺ brine at four concentrations, 0.02 wt%, 0.05 wt%, 0.08 wt%, and 0.10 wt%, and the injection of nanofluids increased the oil recovery by 4% over the low-salinity water flooding. The increase in oil recovery was observed when the nanoparticle concentration increased up to 0.05 wt% and no further increment in oil recovery was observed at nanoparticle concentrations higher than 0.05 wt%. The addition of SiO₂ nanoparticles would increase the viscosity of the injection water and decrease the contact angle between water and oil, but had no significant effect on IFT values. This led to an incremental oil recovery when the low-salinity SiO₂ nanofluid was as a displacing fluid.

Open Access This article is distributed under the terms of the Creative Commons Attribution 4.0 International License (<http://creativecommons.org/licenses/by/4.0/>), which permits unrestricted use, distribution, and reproduction in any medium, provided you give appropriate credit to the original author(s) and the source, provide a link to the Creative Commons license, and indicate if changes were made.

References

- Alotaibi MB, Azmy R, Nasr-El-Din HA. A comprehensive EOR study using low salinity water in sandstone reservoirs. In: SPE improved oil recovery symposium, 24–28 April, Tulsa, Oklahoma, USA, 2010. <https://doi.org/10.2118/129976-MS>.
- Arab D, Pourafshary P. Nanoparticles-assisted surface charge modification of the porous medium to treat colloidal particles migration induced by low salinity water flooding. *Colloids Surf A Physicochem Engi Asp*. 2013;436:803–14. <https://doi.org/10.1016/j.colsurfa.2013.08.022>.
- Arab D, Pourafshary P, Ayatollahi S. Mathematical modeling of colloidal particles transport in the medium treated by nanofluids: deep bed filtration approach. *Transp Porous Media*. 2014;103(3):401–19. <https://doi.org/10.1007/s11242-014-0308-5>.
- Austad T, Rezaeidoust A, Puntervold T. Chemical mechanism of low salinity water flooding in sandstone reservoirs. In: SPE symposium on improved oil recovery, 24–28 April, Tulsa, Oklahoma, USA; 2010. <https://doi.org/10.2118/129767-MS>.
- Ayatollahi S, Zerafat MM. Nanotechnology-assisted EOR techniques: new solutions to old challenges. In: SPE international oilfield nanotechnology conference and exhibition, 12–14 June, Noordwijk, the Netherlands, 2012. <https://doi.org/10.2118/157094-MS>.
- Baird JC, Walz JY. The effects of added nanoparticles on aqueous kaolinite suspensions: II. Rheological effects. *J Colloid Interface Sci*. 2007;306(2):411–20. <https://doi.org/10.1016/j.jcis.2006.10.066>.
- Buikema TA, Mair C, Mercer D, Webb KJ, Hewson A, Reddick CE, et al. Low salinity enhanced oil recovery—laboratory to day one field implementation—LoSal EOR into the Clair Ridge Project. In: IOR 2011—16th European symposium on improved oil recovery, 12 April 2011. <https://doi.org/10.3997/2214-4609.201404782>.
- Chengara A, Nikolov AD, Wasan DT, Trokhymchuk A, Henderson D. Spreading of nanofluids driven by the structural disjoining pressure gradient. *J Colloid Interface Sci*. 2004;280(1):192–201. <https://doi.org/10.1016/j.jcis.2004.07.005>.
- Das S, Choi SU, Yu W, Pradeep T. *Nanofluids: science and technology*. Hoboken: Wiley; 2008.
- Engeset B. The potential of hydrophilic silica nanoparticles for EOR purposes: a literature review and an experimental study. MS Thesis. Institute for petroleumsteknologi og anvendt geofysikk, 2012.
- Hendraningrat L, Torsæter O. Effects of the initial rock wettability on silica-based nanofluid-enhanced oil recovery processes at reservoir temperatures. *Energy Fuels*. 2014;28(10):6228–41. <https://doi.org/10.1021/ef5014049>.
- Hilner E, Andersson MP, Hassenkam T, Matthiesen J, Salino PA, Stipp SLS. The effect of ionic strength on oil adhesion in sandstone—the search for the low salinity mechanism. *Sci Rep* 2015;5, Article number: 9933. <https://doi.org/10.1038/srep09933>.
- Huang T, Crews JB, Willingham JR. Nanoparticles for formation fines fixation and improving performance of surfactant structure fluids. International petroleum technology conference, 3–5 December, Kuala Lumpur, Malaysia, 2008. <https://doi.org/10.2523/IPTC-12414-MS>.
- Lager A, Webb K, Black C. Impact of brine chemistry on oil recovery. In: IOR 2007-14th European symposium on improved oil recovery. 22 April 2007.
- Lager A, Webb KJ, Black CJJ, Singleton M, Sorbie KS. Low salinity oil recovery: an experimental investigation. *Petrophysics*. 2008a;49(01):28–35.
- Lager A, Webb KJ, Collins IR, Richmond DM. LoSal enhanced oil recovery: evidence of enhanced oil recovery at the reservoir scale. In: SPE symposium on improved oil recovery, 20–23 April, Tulsa, Oklahoma, USA; 2008b. <https://doi.org/10.2118/113976-MS>.

- Li R, Jiang P, Gao C, Huang F, Xu R, Chen X. Experimental investigation of silica-based nanofluid enhanced oil recovery: the effect of wettability alteration. *Energy Fuels*. 2016;31(1):188–97. <https://doi.org/10.1021/acs.energyfuels.6b02001>.
- Ligthelm DJ, Gronsveld J, Hofman J, Brussee N, Marcelis F, van der Linde H. Novel water flooding strategy by manipulation of injection brine composition. In: EUROPEC/EAGE conference and exhibition, 8–11 June, Amsterdam, the Netherlands; 2009. <https://doi.org/10.2118/119835-ms>.
- Matthiesen J, Bovet N, Hilner E, Andersson MP, Schmidt DA, Webb KJ, et al. How naturally adsorbed material on minerals affects low salinity enhanced oil recovery. *Energy Fuels*. 2014;28(8):4849–58. <https://doi.org/10.1021/ef500218x>.
- Mcelfresh PM, Holcomb DL, Ector D. Application of nanofluid technology to improve recovery in oil and gas wells. In: SPE international oilfield nanotechnology conference and exhibition, 12–14 June, Noordwijk, The Netherlands; 2012. <https://doi.org/10.2118/154827-MS>.
- Morrow NR, Buckley J. Improved oil recovery by low-salinity water flooding. *J Pet Technol*. 2011;63(05):1066–112. <https://doi.org/10.2118/129421-MS>.
- Nasralla RA, Nasr-El-Din HA. Double-layer expansion: is it a primary mechanism of improved oil recovery by low-salinity water flooding? *SPE Reserv Eval Eng*. 2014;17(1):49–59. <https://doi.org/10.2118/154334-PA>.
- Piñerez Torrijos ID, Puntervold T, Strand S, Austad T, Abdullah HI, Olsen K. Experimental study of the response time of the low-salinity enhanced oil recovery effect during secondary and tertiary low-salinity water flooding. *Energy Fuels*. 2016;30(6):4733–9. <https://doi.org/10.1021/acs.energyfuels.6b00641>.
- Pourafshary P, Azimpour SS, Motamedi P, Samet M, Taheri SA, Bargozin H, et al. Priority assessment of investment in development of nanotechnology in upstream petroleum industry. In: SPE Saudi Arabia section technical symposium, 9–11 May, Al-Khobar, Saudi Arabia, 2009. <https://doi.org/10.2118/126101-MS>.
- Qiao C, Johns R, Li L. Modeling low-salinity water flooding in chalk and limestone reservoirs. *Energy Fuels*. 2016;30(2):884–95. <https://doi.org/10.1021/acs.energyfuels.5b02456>.
- Rahbar M, Ayatollahi S, Ghatee MH. The roles of nano-scale inter-molecular forces on the film stability during wettability alteration process of the oil reservoir rocks. In: Trinidad and Tobago energy resources conference, 27–30 June, Port of Spain, Trinidad; 2010. <https://doi.org/10.2118/132616-MS>.
- Tang GQ, Morrow NR. Influence of brine composition and fines migration on crude oil/brine/rock interactions and oil recovery. *J Pet Sci Eng*. 1999;24(2):99–111. [https://doi.org/10.1016/S0920-4105\(99\)00034-0](https://doi.org/10.1016/S0920-4105(99)00034-0).
- Timofeeva EV, Moravek MR, Singh D. Improving the heat transfer efficiency of synthetic oil with silica nanoparticles. *J Colloid Interface Sci*. 2011;364(1):71–9. <https://doi.org/10.1016/j.jcis.2011.08.004>.
- Vledder P, Gonzalez IE, Carrera Fonseca JC, Wells T, Ligthelm DJ. Low salinity water flooding: proof of wettability alteration on a field wide scale. In: SPE symposium on improved oil recovery, 24–28 April, Tulsa, Oklahoma, USA; 2010. <https://doi.org/10.2118/129564-MS>.
- Wasan DT, Nikolov AD. Spreading of nanofluids on solids. *Nature*. 2003;423(6936):156. <https://doi.org/10.1038/nature01591>.
- Wasan DT, Nikolov A, Kondiparty K. The wetting and spreading of nanofluids on solids: role of the structural disjoining pressure. *Curr Opin Colloid Interface Sci*. 2011;16(4):344–9. <https://doi.org/10.1016/j.cocis.2011.02.001>.
- Xie Q, Liu Y, Wu J, Liu Q. Ions tuning water flooding experiments and interpretation by thermodynamics of wettability. *J Pet Sci Eng*. 2014;124:350–8. <https://doi.org/10.1016/j.petrol.2014.07.015>.
- Zamani A, Maini B, Pereira-Almao P. Experimental study on transport of ultra-dispersed catalyst particles in porous media. *Energy Fuels*. 2010;24(9):4980–8. <https://doi.org/10.1021/ef100518r>.
- Zhang TT, Davidson D, Bryant SL, Huh C. Nanoparticle-stabilized emulsions for applications in enhanced oil recovery. In: SPE improved oil recovery symposium, 24–28 April, Tulsa, Oklahoma, USA; 2010. <https://doi.org/10.2118/129885-MS>.